Journal of Porous Materials (2023) 30:2101–2112
https://doi.org/10.1007/s10934-023-01489-1

Development of polyimide aerogel stock shapes through polyimide aerogel particles

Shima Dayarian[1] · Liu Yang[1] · Hojat Majedi Far[2]

Accepted: 26 May 2023 / Published online: 9 June 2023
© Crown 2023

Abstract
Polyimide aerogels have excellent thermal and mechanical properties, resulting in various applications, especially in insulation areas. However, the conventional methods for directly producing aerogel blocks can be time-consuming and expensive due to the long-term solvent exchange and drying. This study developed two alternative techniques, adding dimethyl sulfoxide solvent and epoxy into the polyimide aerogel particles and consolidating them to obtain PI aerogel blocks or stock shapes. This approach reduced the cycle time of the process by nearly 60% compared to the directly obtained stock shapes. Samples with epoxy look promising in appearance and mechanical properties compared to the stock shapes made directly. The compression test shows that adding epoxy improves the mechanical property and compressive strength at 10% strain by 18%. In the same context, the samples made using dimethyl sulfoxide as a solvent exhibit higher thermal stability and porosity when compared to directly made stock shapes. These techniques provide a range of good thermal and mechanical properties for polyimide aerogel stock shapes prepared from the particles.

Keywords Polyimide aerogel · Stock shape · Porosity · Thermal stability · Thermal conductivity · Mechanical properties · Ambient pressure drying · Consolidation

1 Introduction

Polyimide (PI) aerogels exhibit low density, high internal surface area, excellent mechanical and thermal stability, low thermal conductivity, and low dielectric constant [1–3]. These attributes make them an ideal candidate for insulation solutions in aerospace components and various other technologies [4], such as lightweight substrates for high-performance antennas [5], building insulation [6], thermal insulation for cryogenic propellant tanks [7], and flexible insulation for space suits, inflatable structures for entry, descent, and landing [8]. Although linear polyimide aerogels have mechanical properties on par with other polymers with similar densities, they experience significant shrinkage during the drying process. In contrast, cross-linked PI aerogels can help withstand shrinkage in drying and maintain a porous structure [9]. Among various methods developed for synthesizing PI aerogels, the most versatile may be cross-linking amine-terminated with anhydride-terminated oligomers [10].

Preparation of the cross-linked PI aerogels typically involves two steps: (i) wet-gel formation using sol–gel method [11] and (ii) drying the wet gel in several different ways [1, 10, 11]. The wet gel needs to go through a solvent exchange step before drying. Highly porous PI aerogels obtained can be flexible thin films [12] or powders [13]. Besides those forms, they can take the shape of their moulding vessel used during gelation, thus forming various desired shapes such as rectangular, cubic, cylindrical, and so on. The latter forms are referred to as aerogel blocks or *stock shapes*.

The solvent exchange for the PI stock shapes requires significant time and solvents, making the process costly, especially on a large scale. For example, Lee et al. investigated the effect of different solvents on solvent exchange steps. They applied solvents exchange 6 times every 2 h, resulting in a total of 12 h [1]. Ghaffari et al. worked on synthesizing the polyimide aerogel using 3,3',4,4'-biphenyl tetracarboxylic dianhydride (BPDA) and pyromellitic dianhydride (PMDA). The method used for the solvent exchange

✉ Shima Dayarian
s.dayarian@strath.ac.uk

[1] Department of Mechanical and Aerospace Engineering, University of Strathclyde, 75 Montrose Street, Glasgow G1 1XJ, UK

[2] Blueshift Materials Inc., Spencer, MA 01562, USA

in their study took 6 days [14]. Blueshift Materials applied 6 days of solvent exchange to fabricate the polyimide stock shape [14]. A more efficient solvent exchange process will significantly reduce the PI aerogel production cycle and lead to considerable cost-saving. The focus of this work is to minimize the time for solvent exchange and, as a result, reduce the total time and cost for the fabrication of PI stock shapes through first producing PI aerogel particles with an enhanced surface-to-volume ratio. The solvent exchange will be accelerated drastically in the powder particles compared to the PI stock shape counterparts. Although PI aerogel particles can be directly used as a final product, it is desirable to develop a cost-effective process in order to convert PI aerogel particles into stock shapes. To our best knowledge, such an investigation has not been reported for PI aerogel in the literature.

Due to the advantages of excellent chemical and corrosion resistance, thermal and dimensional stability, and excellent mechanical and electrical properties, epoxy resins can be used in a broad range of applications in laminating adhesives, surface coating, and semiconductor encapsulation [15, 16]. Many surface treatments have been developed to increase the adhesion between polyimide and epoxy. Huntrakool et al. investigated the surface reactivity of polyimide with other adhesive materials, such as epoxy. They studied the surface reactivity of four different polyimides using contact angle, flow microcalorimetry, Fourier transform infrared spectroscopy, and X-ray photoelectron spectroscopy [17]. Akhter et al. reviewed the composite of polyimide with epoxy [18]. They produced two types of polyimides, blended them with epoxy to make the epoxy-amine network (0–7.5 wt% PI), and characterized them with thermogravimetric analysis (TGA), differential scanning calorimetry (DSC), and x-ray diffraction (XRD). Kim et al. used various techniques to preserve the aerogel pores from resin infiltration. In their method, ethanol was added to fill the pores. They showed that the thermal conductivity of the preserved aerogel pores decreased as the aerogel volume fraction was increased in the composites [19]. Zuo et al. manufactured PI nanofibrous membranes using electrospinning and reinforced them with epoxy resin. Using different characterization methods, they showed that the strength and elongation at break were four times stronger at the contact points, with a fusion of fibers [20]. Piljae et al. made polyimide/acrylic/epoxy bricks using 3D printing techniques. They used this method to manufacture a complex shape sample that was difficult to produce using the supercritical process [21]. As a summary some of the previous work for making the PI aerogel stock shape are presented in Table S1. This literature confirms that changing the solvent takes much time and material for most of the previous work which will be adjusted using the introduced method in this work. In addition, most of the previous work applied supercritical drying which cannot be used in the industrial scale due to usage of high pressure and cost.

In this work, we have investigated the consolidation method for manufacturing PI aerogel stock shapes from aerogel particles instead of direct synthesis and applied ambient pressure drying instead of supercritical drying, which has widely been used for aerogel fabrication. Before the consolidation, PI aerogel particles were treated by either mixing with dimethyl sulfoxide (DMSO) or epoxy resin. The thermal and mechanical properties of these stock shapes were then compared.

2 Experimental

2.1 Materials

All reagents and solvents were used as received. DMSO (≥ 99% Reagent Plus), 4,4'-oxydianiline (ODA), 3,3',4,4'-biphenyltetracarboxylic dianhydride (BPDA), acetone (technical grade), Chloroform, benzoic anhydride (BA), and 2-methyl imidazole (2-MI, 99%) were purchased from Sigma Aldrich. 4,4'-diamino-2,2'-dimethylbiphenyl (DMB), and 1,3,5-Tris(4-aminophenoxy) benzene (TAPOB) were purchased from Tokyo Chemical Industry. IN2 epoxy infusion resin was purchased from Easy Composites. The resin was a mixture of bisphenol-A-epoxy resin and epichlorohydrin-formaldehyde phenol polymer.

2.2 PI aerogel particles

The PI aerogel particles were first synthesized, by following a method used by Blueshift Materials [22], using DMSO as the solvent; DMB, ODA, as diamines; BPDA as a dianhydride and TAPOB as a branching agent. 2-MI and BA were added as catalyst and dehydrating agents, respectively, and the mixture was mixed for 6 min. When a clear yellow solution appeared at the end of 6 min, the sol was poured into a mould. The gelation was recorded to be 30 min. The gel was left in the same mould and aged in ambient conditions for 18–24 h. Subsequently, the gel was washed with acetone six times every 24 h. Finally, the monolithic PI was dried at 200 °C for 90 min under a vacuum and then heated to 300 °C for 12 h under an argon flow. The whole process of making the stock shape in the direct process took more than 8 days. The PI stock shape was then milled with a CAMaster-Stinger I dry miller machine with a feed rate of 50 in/min, plunge rate of 15 in/min, and rotational speed of 12,000 rpm. The obtained PI aerogel particles are shown in Fig. 1 a, b presents the microstructure of these particles using scanning electron microscopy (SEM).

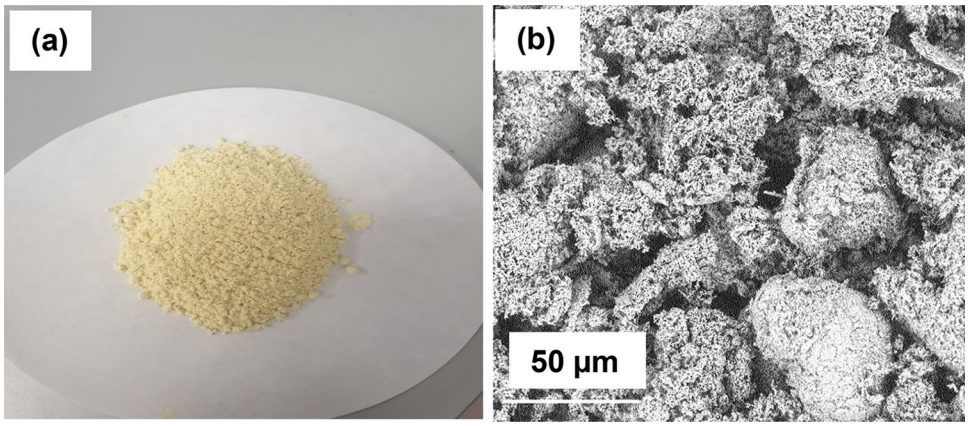

Fig. 1 **a** A photograph and **b** SEM of PI aerogel particles used in the present work as received

2.3 Treatment of PI aerogel particles

This work used two methods to treat the PI aerogel particles, including (i) varying the amount of DMSO and (ii) epoxy resin. The samples made using these methods are referred to as PI-DMSO-X or PI-epoxy-X, where the X refers to either the % mass of DMSO or epoxy mixed with PI aerogel particles.

2.4 Incorporation of DMSO

Turning PI aerogel particles into a porous stock shape requires PI particles to be consolidated without significantly losing the porosity in the particles. It is believed that adding DMSO would wet PI aerogel particles, making them more prone to be stuck together during the moulding process, thus reducing the tendency of crushing particles by consolidation. The DMSO was chosen for compatibility with the monomers and particles, as it is the original solvent for the PI aerogel synthesis. It was added to the particle system in different contents: 0.0, 3.0, 5.0, 10 and 30% mass with respect to the total mass of the particles; see Fig. 2a. Acetone was then added, and the mixtures were manually stirred for 5 min to yield a uniform dispersion, as shown in Fig. 2b. The mixture was left overnight to evaporate the extra acetone. The remaining mixture was finally moulded and fully dried at 250 °C for 24 h according to the direct method of aerogel block preparation [12].

2.5 Incorporation of epoxy

A water-particle slurry was created by adding 20 ml of water to 1 g of PI aerogel particles. The slurry was shaken vigorously to ensure complete mixing between the water and particles, as shown in Fig. 3a. Due to its viscose nature, epoxy cannot be well mixed with PI aerogel particles directly. In order to achieve a uniform epoxy dispersion around individual particles, epoxy was dispersed in chloroform before adding into the particles. Two different parts of the epoxy (resin and hardener), at a stoichiometric ratio of 100:30 by weight, were mixed with chloroform manually in a separate container. For each 5 g of the particles, 20 ml chloroform was added to epoxy, which was added in 3.0, 5.0, 9.0, and 20% mass with respect to the total mass of the particles. Next, the dispersed epoxy mixture was introduced into the water-particle slurry and mixed manually for 10 min. The produced mixture was left in ambient condition for 24 h to evaporate the excess water, as shown in Fig. 3b. Finally, the mixture was filtered using a Buchner funnel and an aspirator setup and was ready for moulding (Fig. 3c).

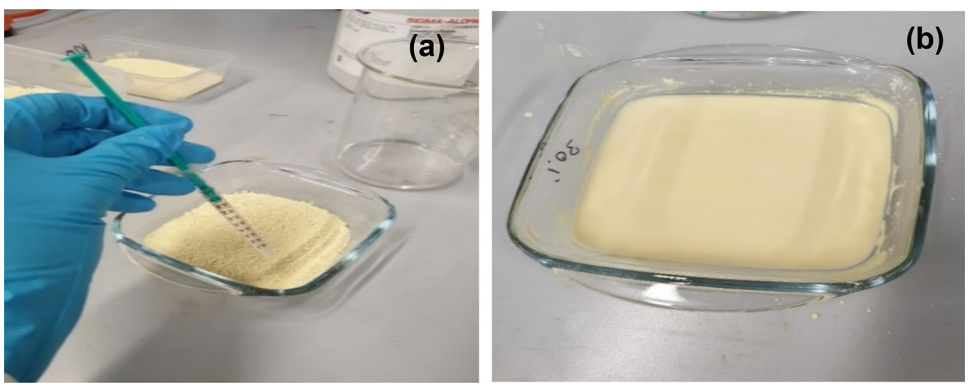

Fig. 2 The steps involved in the incorporation of DMSO into the PI aerogel particles: **a** the addition of DMSO to PI aerogel particles and **b** the mixture of the particle with DMSO after the addition of acetone

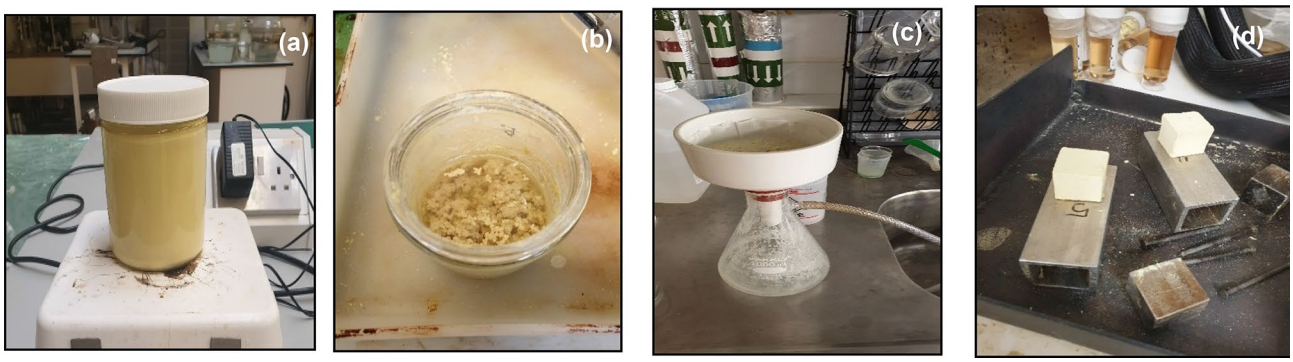

Fig. 3 The steps involved in the incorporation of epoxy into the PI aerogel particles: **a** the slurry mixture of water-PI aerogel particles; **b** the mixture after the addition of epoxy, and **c** after filtering the mixture of water-PI-epoxy, **d** demoulded PI aerogel stock shape

2.6 Particle consolidation

Conversion of PI aerogel particles to the stock shapes was carried out through consolidation moulding. First, an aluminium tube with an internal area of 1×1 inch was machined. Two aluminium blocks were machined, slid inside the tube, and secured by pins through open holes on the tube side. The distance between the two blocks was 1 inch, and consequently, a $1 \times 1 \times 1$ inch cavity was created inside the tube. The PI aerogel particles treated with DMSO or epoxy were then transferred into this cavity. 4.5 g of the particles were used in order to ensure the particle bulk volume was greater than 1 cubic inch so that when the blocks were put in place, the particles were under compression. The particle-filled mould was then transferred to an oven, where the DMSO-treated particles were heated at 250 °C for 24 h (to remove all the added DMSO during the drying process), and epoxy-treated particles were heated at room temperature for 24 h and 80 °C for 6 h. This temperature and method were selected based on the curing condition for the applied epoxy by its supplier. Stepwise drying was used for these samples in order to control the viscosity increment and reduce any chance of infiltration of the epoxy inside the pores.

The final step was demoulding the sample carefully and obtaining stock shape samples, as shown in Fig. 3d. Figure S1 shows a schematic process for making the stock shape samples at this work.

3 Material characterization

The thermal stability of the stock shape samples was measured by thermogravimetric analysis (TGA) using a TA Instruments Q50 thermogravimetric analyzer.13–20 mg of PI aerogel stock shapes were used in each test, and the temperature was increased from 20 to 700 °C under air at a heating rate of 10 °C/min. The temperatures corresponding to 10% weight loss, rate of weight loss and weight loss onset were recorded.

Brunauer–Emmett–Teller (BET) specific surface areas were obtained by nitrogen sorption at 77 K using a Micromeritics ASAP2420 [23, 24]. The desorption branch of the isotherms was used to obtain the Barrett-Joyner-Halenda (BJH) pore size distributions [24]. Before the analysis, approximately 0.2 g of the sample was subjected to a degas cycle of 30 min at 50 °C, followed by 120 min at 120 °C, at a pressure of 10 mmHg.

The complete pore size distributions were determined using mercury intrusion porosimetry (MIP) with a Quantachrome Poremaster system. Approximately 0.1 g of the sample was placed into a penetrometer for low and high-pressure analysis. After adding the high-pressure jacket, the high-pressure stage measured the mercury intruded/extruded volume up to 60000 psi.

Bulk densities (ρ_b) were measured using the mass and volume of the samples for an average of three specimens per sample. Skeletal densities (ρ_s) were measured using a Micromeritics Accupyc II 340 helium pycnometer with 50 fill/ vent cycles on a single sample. The % porosities were calculated using [25]:

$$\% \text{ Porosity } = 100 \times \left[\left(\rho_s - \rho_b\right)/\rho_s\right] \quad (1)$$

The compression properties of the samples were undertaken by an Instron 5969 series universal testing system equipped with a video extensometer followed by ASTM D1621. The equipment was fitted with a 50 kN load cell to evaluate the effect of the DMSO and epoxy on the particle-converted stock shapes. The cubic stock shapes with the dimensions of $25 \times 25 \times 25$ mm at a constant rate of 0.65 mm/min at room temperature were tested.

A XIATECH TC3000E thermal conductivity meter was used to measure the thermal conductivity of the samples, according to ASTM C1113. A 1 V heating voltage hot wire sensor was placed between the samples. Before analyzing

the samples, a polymethyl methacrylate (PMMA) standard sample was tested to calibrate the instrument. For all measurements, a 500 g deadweight was placed on the sample to provide pressure and keep the sample in good contact with the sensor surface.

4 Results and discussion

The weight changes and rates of weight change against temperature for PI-DMSO samples are plotted in Fig. 4. It can be seen in Fig. 4a that there is no weight loss until the temperature reaches 430 °C for both neat PI and PI-DMSO stock shapes. The overlapping of small peaks can further confirm this at 430 °C for all samples in Fig. 4b. From 430 to 540 °C, thermal degradation accelerates in all samples. Between 540 and 590 °C, samples loss most of their weight. From the rate of weight change, it can be observed that the neat PI is slightly more thermal stable as it has the lowest weight loss rate compared to PI-DMSO samples. In all PI-DMSO samples, degradation was completed at 670 °C. Adding different concentrations of DMSO did not significantly impact the thermal decomposition. As mentioned, the reason to treat already synthesized PI particles with DMSO solvent is to soften the PI aerogel particles. This solvent is expected to be removed through the drying process implemented in this work.

The minimum onset point is 540 °C in PI-DMSI-10 sample. As there is no significant weight loss before the decomposition point, it can be confirmed that DMSO level was significantly reduced during the subsequent drying. The 10% weight loss and the onset temperatures are also summarized along with other characterized properties in Table 1.

For PI-epoxy samples, as can be seen in Fig. 5, the weight loss generally starts around 200 °C. The rate of weight change has two primary peaks: one at 350 °C and the other between 540 and 580 °C. Between these two peaks, weight loss takes place at a lower rate. As the % epoxy increases in the samples, the thermal stability decreases monotonically. In fact, by increasing the concentration of the epoxy from 0 to 100 wt%, the temperature for 10% weight loss dropped by 40%.

On the other hand, the imidization process can be investigated using the TGA results. The imidization generally consists of evaporating the solvent and cyclodehydration, followed by weight loss in the samples with incomplete imidization. The imidization usually occurs between 100 and 200 °C [26]. Samples obtained from both methods do not experience a noticeable weight loss up to 200 °C, confirming that the solvent is removed and the imidization is completed during the preparation and drying [27]. These results are in good agreement with the thermal studies of polyimide aerogels [8, 28].

Comparing the measured onset points for stock shapes at various DMSO and epoxy levels indicates no massive change (Tables 1 and 2). The thermal stability of the polymer material mainly depends on the chemistry and concentration of the monomers [4]. Therefore, no noticeable weight change can be observed by increasing the concentration of either DMSO or epoxy for both methods. In addition, comparing the 10% decomposition temperatures of all samples, PI-DMSO samples show thermal stabilities as high as the directly fabricated stock shape (see Tables 1–2).

Figures 6 and 7 present the pore size distributions for PI-DMSO and PI-epoxy samples using nitrogen sorption and MIP, respectively. Figure 6a shows the average size of the pores measured by nitrogen sorption (77 K) for PI-DMSO samples is between 20 and 37 nm. The presence of pores between 900 and 3000 nm and the bimodal distributions for all DMSO levels in Fig. 6b indicate that the pores are mostly mesopores and macropores. The directly made PI stock shape shows a sharp, narrow single peak in 300 to 700 nm. This peak confirms that the pores in this sample are smaller and more uniform than the pores in the PI-DMSO samples. The MIP median pore diameter for directly prepared stock shape is 0.606 μm, smaller than the PI-DMSO samples (see Table 2).

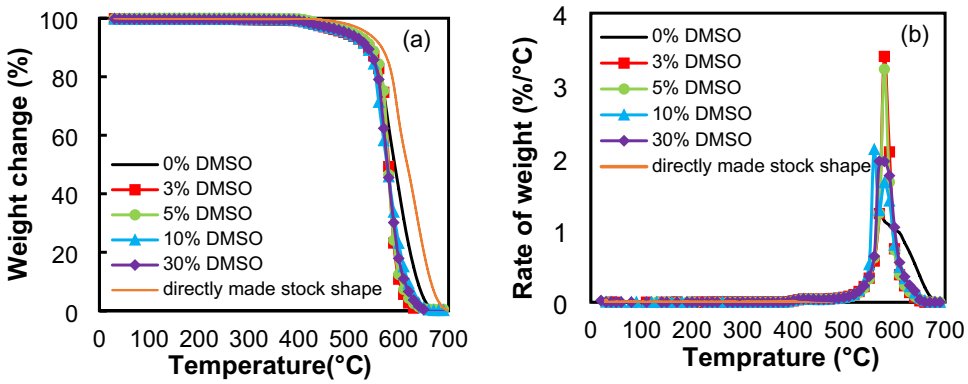

Fig. 4 **a** Weight (%), and **b** rates of weight change as a function of temperature for PI-DMSO samples

Table 1 Critical materials properties of PI stock shapes

% mass of DMSO or epoxy	Bulk Density (g/cm^3)[a] ρ_b	Skeletal density (g/cm^3)[b] ρ_s	Porosity (%)[c]	BET surface area (m^2/g)[d]	MIP median pore diameter (μm)[e]	TGA (10%) (°C)[f]	TGA onset temperature (°C)	Compressive modulus (MPa)[g]	Compressive strength, 10% strain (MPa)[h]	Thermal conductivity (W/m. K)[i]
PI-DMSO stock shapes										
0	0.27 ± 0.04	1.49 ± 0.02	78.8 ± 4.7	$7.7 \pm 0.0_3$	1.110 ± 0.022	545	550	17.80 ± 0.02	–	0.056 ± 0.001
3	0.28 ± 0.02	1.50 ± 0.01	80.9 ± 1.4	8.0 ± 0.1	1.360 ± 0.006	535	563	14.24 ± 0.04	–	0.054 ± 0.002
5	0.25 ± 0.01	1.50 ± 0.01	81.7 ± 0.2	8.5 ± 0.1	1.391 ± 0.071	545	567	12.92 ± 0.25	–	0.052 ± 0.003
10	0.24 ± 0.05	1.47 ± 0.01	82.6 ± 1.4	8.6 ± 0.1	1.570 ± 0.206	535	567	11.85 ± 0.11	–	0.051 ± 0.004
30	0.22 ± 0.01	1.49 ± 0.01	88.8 ± 1.5	$8.4 \pm 0.0_1$	2.110 ± 0.102	535	541	10.70 ± 0.50	–	0.050 ± 0.003
PI-epoxy stock shapes										
0	0.32 ± 0.02	1.48 ± 0.01	66.5 ± 2.3	8.9 ± 0.1	1.201 ± 0.302	530	541	2.30 ± 1.30	–	0.052 ± 0.005
3	0.37 ± 0.01	1.48 ± 0.01	73.6 ± 5.3	9.5 ± 0.1	0.760 ± 0.011	520	556	23.30 ± 3.50	0.99	0.065 ± 0.002
5	0.40 ± 0.01	1.44 ± 0.01	71.0 ± 1.2	13.1 ± 2.1	0.861 ± 0.015	500	553	43.20 ± 4.31	2.19	0.078 ± 0.001
9	0.35 ± 0.01	1.46 ± 0.01	81.1 ± 1.1	14.3 ± 1.2	1.060 ± 0.108	390	547	42.10 ± 0.10	0.78	0.077 ± 0.005
20	0.33 ± 0.01	1.42 ± 0.01	84.8 ± 0.7	$7.9 \pm 1.0_1$	1.190 ± 0.229	320	524	32.20 ± 0.10	0.13	0.069 ± 0.001

The authors declare that they have no known competing financial interests or personal relationships that could have appeared to influence the work reported in this paper. % mass of DMSO or epoxy

[a]Using mass (m) and volume (v) of the samples ($\rho = m/v$), average of three samples

[b]50 Cycles on a single sample using helium pycnometry

[c]Via $100 \times [(\rho_s - \rho_b)/\rho_s]$

[d]Using nitrogen sorption at 77 K, average of three samples

[e]Average of two samples

[f]Temperatures corresponding to 10% weight loss

[g]Slope of elastic part in stress–strain curves, average of three samples

[h]Compressive strength could not be measured at 10% compressive strain for samples with DMSO as the samples disintegrated earlier

[i]Average of two samples using hot wire (ASTM C1113)

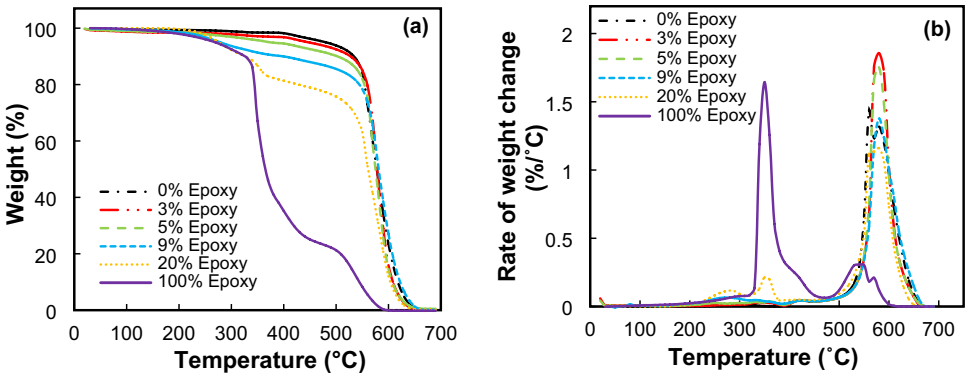

Fig. 5 **a** Weight (%) **b** rates of weight change as a function of temperature for PI-epoxy samples

Table 2 Critical materials properties of directly made PI stock shape

Bulk density (g/cm^3)[a] ρ_b	Skeletal density (g/cm^3)[b] ρ_s	Porosity (%)[c]	MIP median pore diameter (μm)	TGA (10%) (°C)[d]	Compressive modulus (MPa)[e]	Compressive strength, 10% strain (MPa)	Thermal conductivity (W/m.K)[f]
0.23	1.47	84.7	0.606	550	21.00	1.80	0.054 ± 0.005

[a]Using MIP

[b]50 Cycles on a single sample using helium pycnometry

[c]Via $100 \times [(\rho_s — \rho_b) / \rho_s]$

[d]Temperatures corresponding to 10% weight loss

[e]Slope of elastic part in stress–strain curves, average of three measurements

[f]Average three measurements using hot wire

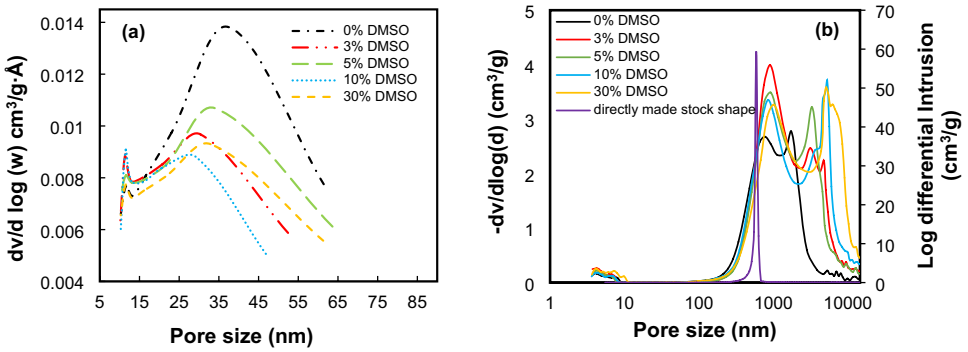

Fig. 6 Pore size distribution for PI-DMSO samples using **a** BJH method from nitrogen sorption and **b** MIP

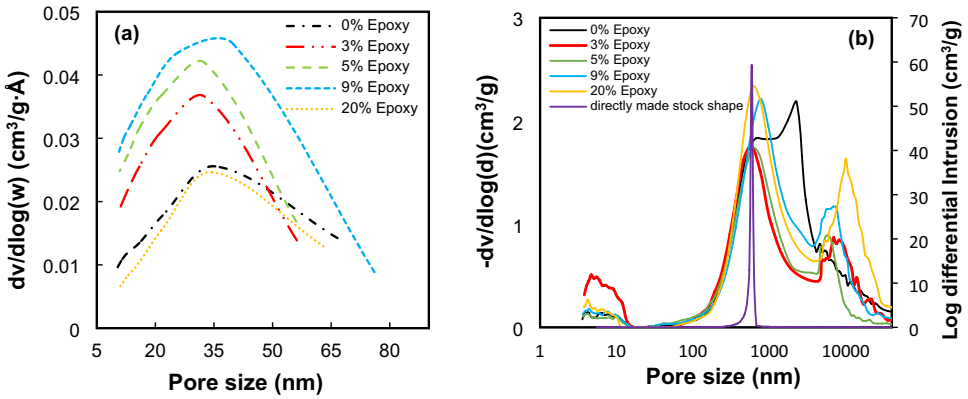

Fig. 7 Pore size distribution for PI-epoxy samples using **a** BJH method from nitrogen sorption, and **b** MIP

As shown in Fig. 7a, the average pore sizes probed by nitrogen sorption for PI-epoxy samples are between 24 and 35 nm, within the same range of values for PI-DMSO samples. PI-epoxy samples also show bimodal pore size distributions (Fig. 7b). The volume of the adsorbed nitrogen for PI-epoxy samples is higher than the DMSO ones.

The BET surface areas of the samples are between 8 and 14 m^2/g. Unsurprisingly, the surface areas of PI aerogels in this study are low compared to that of PI aerogels in the literature. For instance, Kwon et al. showed that the surface area of polyimide aerogel is 103 m^2/g, which is almost 87% higher than PI samples in this work [29]. Feng et al. also presented that the BET-specific surface area is $320-340$ m^2/g [8]. During the ambient pressure drying, the surface tension between the solvent and pore walls results in shrinkage and reduces the surface area. Most of those studies have used supercritical CO_2 instead of ambient pressure drying to minimize the shrinkage in the pore [8]. Figure 8 shows the nitrogen adsorption–desorption isotherms at 77 K for all samples. The hysteresis loops are apparent in every BET isotherm curve, demonstrating that mesopores exist in all cases. This loop also suggests condensing the gas inside the pores at low-pressure ranges and forming mono and multilayers at higher pressure. The nitrogen adsorption isotherms for both methods rise above $P/P_0 = 0.9$ but do not reach the saturation plateau, indicating that they are type II isotherms. Overall, a very low quantity of gas adsorbed at the early stage of the adsorption, together with the large pores seen in the MIP pore size distributions, proves that macropores are a significant portion of the porosity.

Figure 9 shows the density and porosity correlation with different concentrations of DMSO in PI stock shape samples. As it was explained before, the idea for adding the DMSO is to wet the particles; adding DMSO results in more flexible particles with less stress required to consolidate them. As a result, pores are expected to be intact after compression during moulding, and higher porosity is achieved. Therefore, particles do not break into smaller particles which may be caused by high stress. Table 1 shows different properties for PI-DMSO stock shapes with densities of 0.22–0.28 g/cm^3 having high porosities from 80.9 to 88.8%.

Figure 10 shows the correlation of % porosity with the % epoxy in PI-epoxy samples. As can be seen, the % porosity is increased by increasing the % epoxy, except at 5%. This sample has 0.40 g/cm^3 bulk density, the highest value among all samples (see Table 2).

The SEM images for PI-DMSO samples are shown in Fig. 11. The porous structure can be observed in all concentrations of DMSO. These images confirm that adding more DMSO has created more open porosity in the samples, with the highest value of 88.8% reported for 30% DMSO.

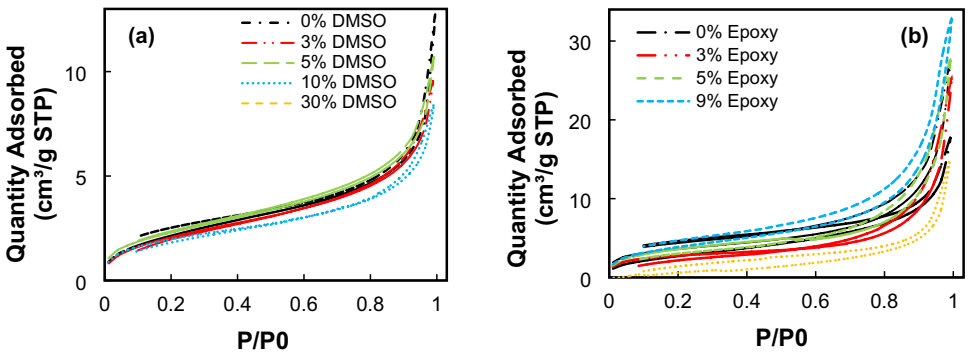

Fig. 8 Nitrogen sorption isotherms at 77 K for **a** PI-DMSO and **b** PI-epoxy samples

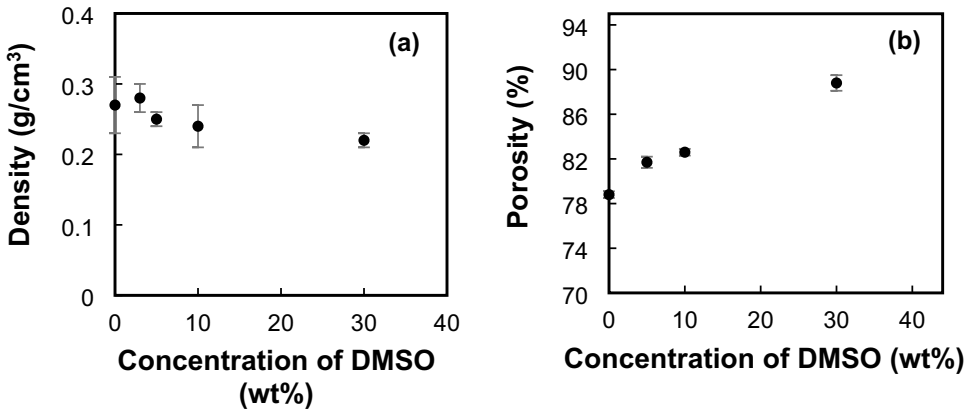

Fig. 9 Correlation of % porosity and density with the % DMSO in PI-DMSO samples

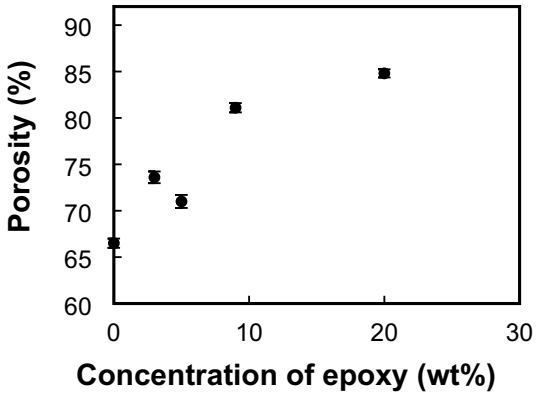

Fig. 10 Porosity-concentration profiles for PI-epoxy stock shapes

The microstructure of the PI-epoxy sample at three different epoxy levels of 0.0, 5.0 and 20%, are shown in Fig. 12. It can be observed that by adding 5.0% epoxy into the particles, a denser structure is shaped compared to the 0% epoxy sample. This could be due to infiltrating the epoxy inside and between the particles. But by adding more epoxy up to 20%, the small pores inside the particles may be filled, and the rest of the epoxy will cover the surface of the particles. Therefore, the bigger particles with lower density will be generated by adding more epoxy from 5 to 20%. The median pore diameters measured with MIP have confirmed these results by showing a 36% increase due to changing the concentration of epoxy from 5 to 20%.

SEM image of the directly prepared PI stock shape shows a porous uniform structure compared to the samples treated with DMSO or epoxy (see Fig. 12d). This sample is 84.7% porous and has 0.23 g/cm^3 bulk density, as shown in Table 2. It is noted that PI-DMSO-30% has almost the same properties as this sample (porosity of 88.8% and density of 0.22 g/cm^3). However, the porous structures are quite different. The directly prepared sample shows a network of tiny particles interconnected throughout the porous structure resembling a fibrous *spider-web-like* structure. In comparison, PI-DMSO and PI-epoxy stock shapes consist of strands formed by randomly bonding larger particles.

Compression tests of the PI stock shapes were carried out to evaluate the effect of DMSO and epoxy treatment on the mechanical performance of the particle-converted PI stock shapes. Compressive modulus was taken as the slope of the elastic domain in the stress–strain curves and are presented in Tables 1 and 2. Adding epoxy and DMSO can significantly affect the mechanical properties of the PI stock shapes. Compressive strength taken as the compressive stress at 10% compressive strain is presented in Table 2 for

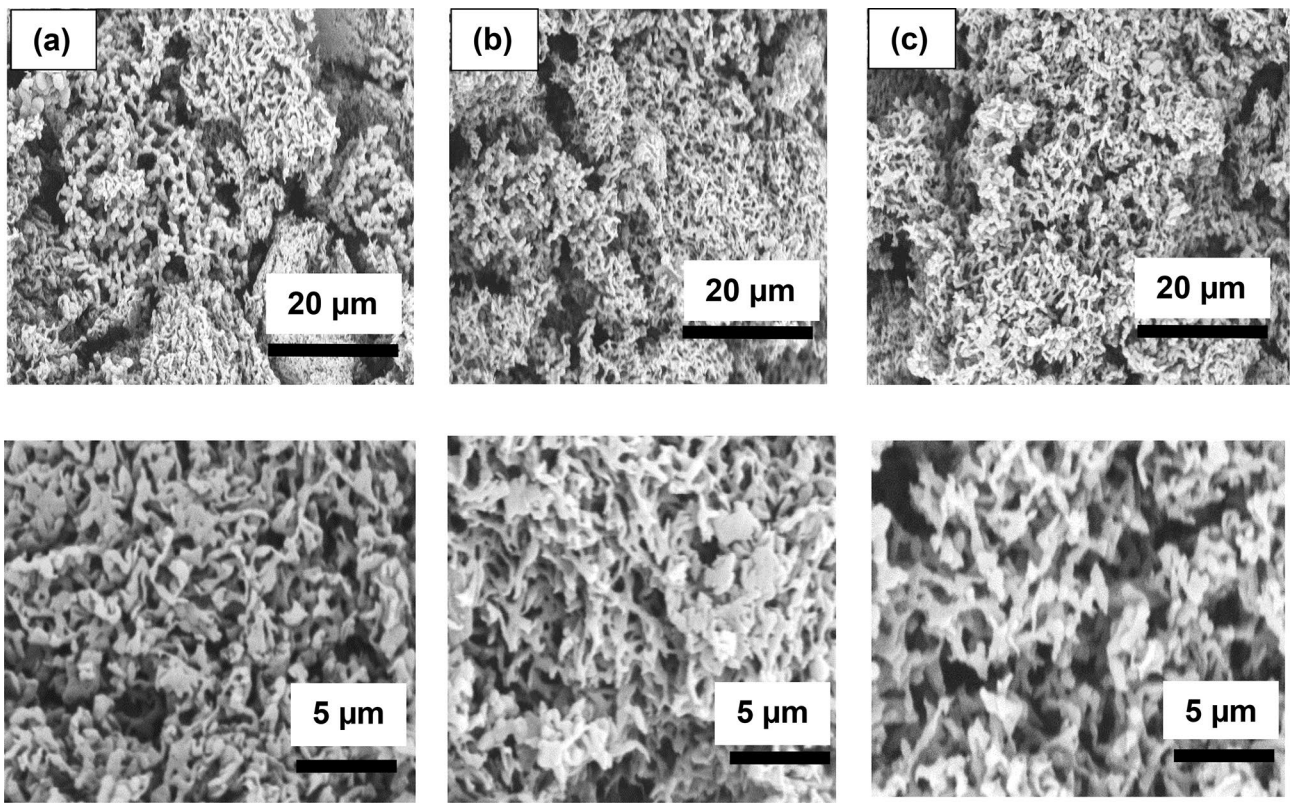

Fig. 11 SEM images of PI-DMSO stock shapes with **a** 0, **b** 5, and **c** 30% DMSO

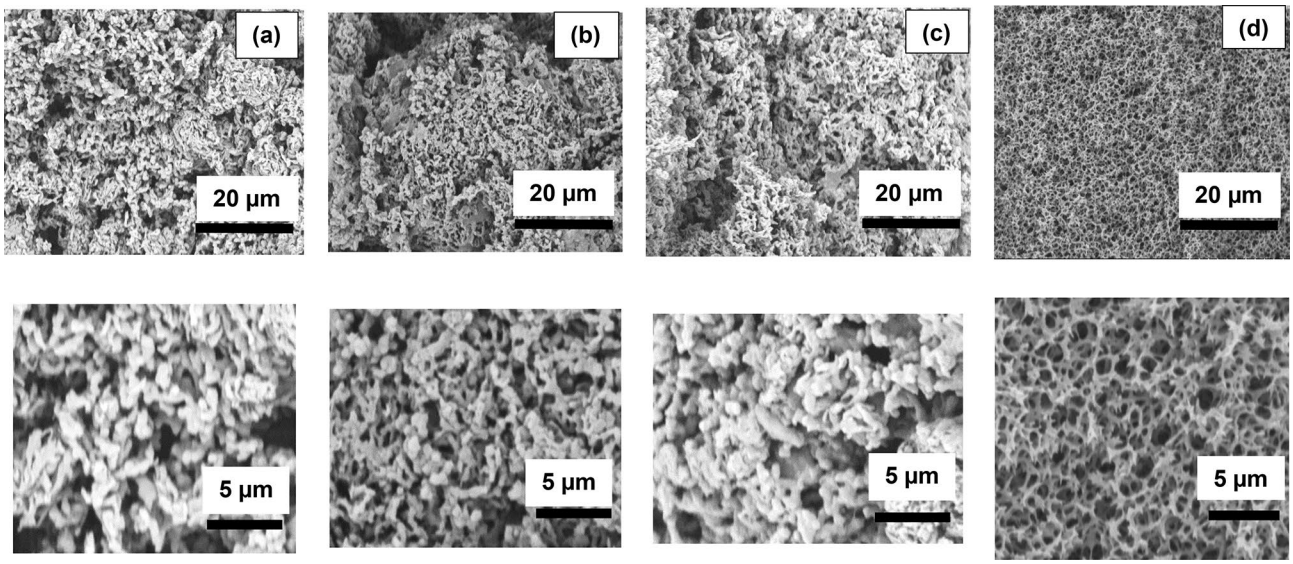

Fig. 12 SEM images of PI-epoxy stock shapes at **a** 0; **b** 5, **c** 20% epoxy, **d** directly made stock shape

stock shapes with epoxy. Compressive strength could not be measured at 10% compressive strain for samples with DMSO as the samples disintegrated earlier. Figure 13 shows the correlation between compressive modulus and DMSO concentration and epoxy concentration. It can be observed that adding DMSO, which increases % porosity and pore size, will reduce the compressive modulus. The PI-DMSO samples with brittle structures were expected to have low mechanical properties.

On the other hand, by increasing the concentration of epoxy up to 5%, the compressive modulus increased up to 43.2 MP and the compressive strength to 2.19 MPa. But then, as was expected from the density and porosity correlation, for PI-epoxy-9 and 20% samples, this value dropped to 42.1 and 32.18 MPa, respectively. This reverse observation could be due to the manufacturing process. For samples with a higher amount of epoxy, there is a chance of sticking the material into the mould's wall; even by using the release agent spray before moulding. Therefore, more force must be applied during moulding and demoulding. It could also be due to the accumulation of excess epoxy between the particles, which weakens the structure. These results are in line with the porosity measurements. Overall, the PI-epoxy samples exhibit higher density, lower porosity, and higher mechanical properties than PI-DMSO samples and PI stock shape made by the direct method.

Figure 14 presents the thermal conductivity of the stock shapes as a function of the % DMSO and % epoxy used to treat the PI aerogel particles. Incorporating DMSO and epoxy into the PI matrix has increased thermal conductivity between 24 and 38% relative to the directly made PI stock shape, as seen in Tables 1 and 2. Figure 14a shows that by increasing the concentration of DMSO, which increases % porosity, the thermal conductivity reduces from 56 to 50 mW/m. K. For PI-epoxy samples, up to 5% epoxy, the thermal conductivity rises to 78 mW/m.K, which is in line with the density and porosity, and then by

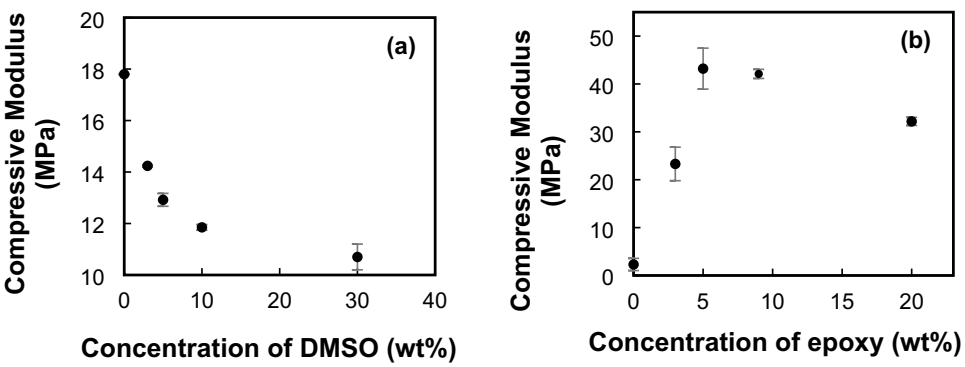

Fig. 13 The compressive modulus of PI stock shapes as a function of the concentration of **a** DMSO and **b** epoxy in the PI aerogel particles

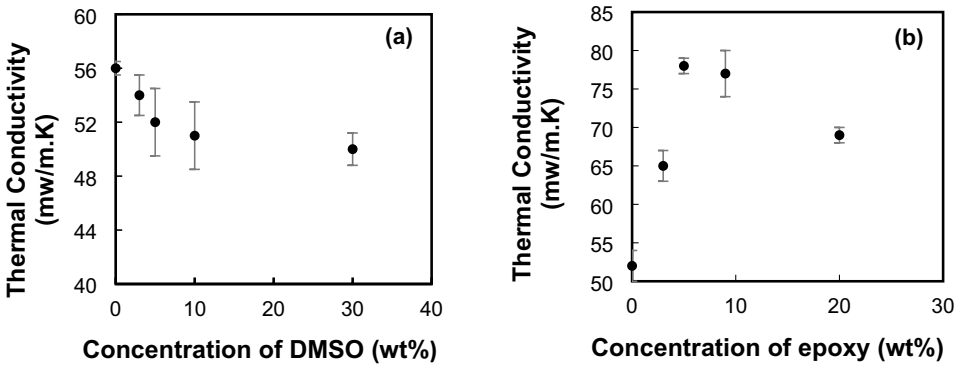

Fig. 14 Thermal conductivity of PI stock shapes as a function of the concentration of **a** DMSO and **b** epoxy in PI aerogel particles

adding more epoxy from 5 to 20%, it drops to 69 mW/m. K, as seen in Fig. 14b.

5 Conclusion

This work has developed a procedure for fabricating PI aerogel stock shapes from consolidation of aerogel particles where DMSO and epoxy systems were used. The original goal of this study was to shorten the production time of aerogel blocks compared to direct stock shape manufacturing. The stock shapes' porous texture and thermal and mechanical properties were investigated. It has been clearly shown that the incorporation of epoxy in the PI aerogel particles (up to 5 wt %) can significantly improve the mechanical properties of the stock shapes. PI-DMSO samples are thermally stable up to 500 °C. On the other hand, the thermal conductivity of the particle-converted stock shapes increases by adding more epoxy due to the infiltration of the pores. Both methods create samples that have pores larger than 50 nm, indicating the presence of macroporosity in their pore structures. However, the densities of stock shapes with epoxy are higher due to the presence of the epoxy between the aerogel particles. The infiltration might have happened despite leaving the mixture before and after moulding at room temperature, resulting in reduced % porosity and increased density. Nevertheless, we have proved that it is feasible to produce PI stock shapes through PI aerogel particles with reasonable thermal and mechanical properties in a shorter time, i.e., ~60 h, compared to the traditional method that is completed in more than 8 days.

Supplementary Information The online version contains supplementary material available at https://doi.org/10.1007/s10934-023-01489-1.

Acknowledgements We would like to express our great gratitude to Blueshift Materials Inc. for their generous support.

Author contributions SD processed the experimental data, manufactured the samples, characterized them, performed the measurements, drafted the manuscript. HM provided the raw material, processed the industrial data and formal analysis. LY supervised the project and reviewed the manuscript. All authors provided critical feedback and helped shape the research and reviewed the manuscript.

Declarations

Conflict of interest The authors declare that they have no known competing financial interests or personal relationships that could have appeared to influence the work reported in this paper.

Open Access This article is licensed under a Creative Commons Attribution 4.0 International License, which permits use, sharing, adaptation, distribution and reproduction in any medium or format, as long as you give appropriate credit to the original author(s) and the source, provide a link to the Creative Commons licence, and indicate if changes were made. The images or other third party material in this article are included in the article's Creative Commons licence, unless indicated otherwise in a credit line to the material. If material is not included in the article's Creative Commons licence and your intended use is not permitted by statutory regulation or exceeds the permitted use, you will need to obtain permission directly from the copyright holder. To view a copy of this licence, visit http://creativecommons.org/licenses/by/4.0/.

8. References

1. D.H. Lee, M. Jung Jo, S.W. Han, S. Yu, H. Park, Polyimide aerogel with controlled porosity: solvent-induced synergistic pore development during solvent exchange process. Polymer (2020). https://doi.org/10.1016/j.polymer.2020.122879
2. Sh. Qiao, Sh. Kang, Z. Hu, J. Yu, Y. Wang, J. Zhu, Moisture-resistance, mechanical and thermal properties of polyimide aerogels. J. Porous Mater. **27**, 237–247 (2020). https://doi.org/10.1007/s10934-019-00801-2
3. X. Hou, Y. Mao, R. Zhang, D. Fang, Super-flexible polyimide nanofiber cross-linked polyimide aerogel membranes for high efficient flexible thermal protection. Chem. Eng. J. (2021). https://doi.org/10.1016/j.cej.2021.129341
4. M.A. Meador, Ch.R. Aleman, K. Hanson, N. Ramirez, S.L. Vivod, N. Wilmoth, L. McCorkle, Polyimide aerogels with amide cross-links: a low cost alternative for mechanically strong polymer aerogels. ACS Appl. Mater. Interfaces **7**(2), 1240–1249 (2015). https://doi.org/10.1021/am507268c
5. Y. Zhong, Y. Kong, J. Zhang, Y. Chen, B. Li, X. Wu, S. Liu, X. Shen, Sh. Cui, Preparation and characterization of polyimide aerogels with a uniform nanoporous framework. Langmuir **34**(36), 10529–10536 (2018). https://doi.org/10.1021/acs.langmuir.8b01756

6. X. Zhang, X. Ni, M. He, Y. Gao, Ch. Li, X. Mo, G. Sun, B. You, A synergistic strategy for fabricating an ultralight and thermal insulating aramid nanofiber/polyimide aerogel. Royal Soc. Chem. **5**, 804–816 (2021). https://doi.org/10.1039/D0QM00724B
7. J.G. Marchetta, F. Sabri, D.S. Williams, D.W. Pumroy, Small-scale room-temperature-vulcanizing-655/aerogel cryogenic liquid storage tank for space applications. J. Spacecr. Rockets (2018). https://doi.org/10.2514/1.A33845
8. J. Feng, X. Wang, Y. Jiang, D. Du, J. Feng, Study on thermal conductivities of aromatic polyimide aerogels. ACS Appl. Mater. Interfaces **8**(20), 12992–12996 (2016). https://doi.org/10.1021/acsami.6b02183
9. Y. Lin, C. Chen, H. Shani, D. Zhang, W. Guozhang, Facile fabrication of mechanically strong and thermal resistant polyimide aerogels with anExcess of cross-linker. J. Mater. Res. Technol. (2020). https://doi.org/10.1016/j.jmrt.2020.07.075
10. Sh.Y. Yang, *Advanced polyimide materials* (Elsevier, Amsterdam, 2018)
11. B. Shi, B. Ma, C. Wang, H. He, Q. Lijie, X. Baosheng, Y. Chen, Fabrication and applications of polyimide nano-aerogels. Compos. A (2021). https://doi.org/10.1016/j.compositesa.2021.106283
12. G. Poe., A. Sakagughi., N. Lambdin., K. Koldan., D. Irvin. Highly Branched Non Crosslinked Aerogel Having Macropores, Methods of Making, and Uses Thereof 2018: United States. WO/2018/200838.
13. S. Dayarian, H. Majedi Far, L. Yang, Macroporous polyimide aerogels: a comparison between powder microparticles synthesized via wet gel grinding and emulsion processes. Langmuir **39**(5), 1804–1814 (2023). https://doi.org/10.1021/acs.langmuir.2c02696
14. Sh. Ghaffari, Z. Saadatnia, F. Shi, Ch.B. Park, H.E. Naguib, Structure to properties relations of BPDA and PMDA backbone hybrid diamine polyimide aerogels. Polymer **176**, 213–226 (2019). https://doi.org/10.1016/j.polymer.2019.05.050
15. C. D. Rutledge. 1961 An Investigation and research regarding the adhesive qualities of epoxy resins in architectural construction. In College of Architecture and Design, Kansas State University
16. D.S. Kut, EPOXY RESIN: surface coatings part one. Anti-Corrosion Meth. Mater. **11**(8), 18–22 (1964). https://doi.org/10.1108/eb020211
17. P. Hoontrakul, R.A. Pearson, Surface reactivity of polyimide and its effect on adhesion to epoxy. J. Adhesion Sci. Technol. **20**(16), 1905–1928 (2006). https://doi.org/10.1163/156856106779116605
18. T. Akhter, H.M. Siddiqi, Z. Akhter, M.S. Butt, Synthesis and characterization of some polyimide-epoxy composites. E-Polymers (2011). https://doi.org/10.1515/epoly.2011.11.1.244
19. S.Y. Kim, Y.J. Noh, J. Lim, N.H. You, Silica aerogel/polyimide composites with preserved aerogel pores using multi-step curing. Macromol. Res. **22**(1), 108–111 (2013)
20. Z.Z. Fan, H.W. He, D. Yuan, L.L. Pang, Y.Z. Huang, Y.Z. Long, X. Ning, Fabrication of epoxy resin reinforced polyimide (PI) nanofibrous membrane. Mater. Lett. **252**, 138–141 (2019)
21. P. Joo, Y. Yao, N. Teo, S.C. Jana, Modular aerogel brick fabrication via 3D-printed molds. Addit. Manuf. (2021). https://doi.org/10.1016/j.addma.2021.102059
22. G. Poe, A. Sakaguchi, N. Lambdin, Highly branched non-crosslinked aerogel, methods of making, and uses thereof. U.S. Patent 10,287,411, 2019
23. M. Naderi, *Surface area: brunauer–emmett–teller (BET)* (In Progress in Filtration and Sepration, Elsevier, Amsterdam, 2015)
24. M. Thommes, K. Kaneko, A.V. Neimark, J.P. Olivier, F. Rodriguez-Reinoso, J. Rouquerol, K.W. Sing, Physisorption of gases, with special reference to the evaluation of surface area and pore size distribution (IUPAC Technical Report). Pure Appl. Chem. **87**(9–10), 1051–1069 (2015). https://doi.org/10.1515/pac-2014-1117
25. M. Maghsoodi, Z. Yari, effect of drying phase on the agglomerates prepared by spherical crystallization. Iran J. Pharm. Res. **14**(1), 51–57 (2015)
26. Y.K. Xu, M.S. Zhan, K. Wang, Structure and properties of polyimide films during a farInfrared-induced imidization process. Polym. Sci. **42**, 2490–2501 (2004). https://doi.org/10.1002/polb.20124
27. Ch. Chidambareswarapattar, Z. Larimore, Ch. Sotiriou-Leventis, J. Mang, N. Leventis, One-step room-temperature synthesis of fibrous polyimide aerogels from anhydrides and isocyanates and conversion to isomorphic carbons. J. Mater. Chem. **20**(43), 9666–9678 (2010). https://doi.org/10.1039/C0JM01844A
28. B.N. Nguyen, M.A.B. Meador, D. Scheiman, L. McCorkle, Polyimide aerogels using triisocyanate as cross-linker. ACS Appl. Mater. Interfaces **9**(32), 27313–27321 (2017). https://doi.org/10.1021/acsami.7b07821
29. J. Kwon, J. Kim, T. Yoo, D. Park, H. Han, Preparation and characterization of spherical polyimide aerogel microparticles. Macromol. Mater. Eng. (2014). https://doi.org/10.1002/mame.201400010

Publisher's Note Springer Nature remains neutral with regard to jurisdictional claims in published maps and institutional affiliations.